

# Development and Implementation of a Micro-electric Discharge Machine: Real-Time Monitoring System of Fabrication of Nanosilver Colloid

Kuo Hsiung Tseng<sup>1</sup> · Yi-Syuan Kao<sup>1</sup> ·  
Chaur-Yang Chang<sup>1</sup>

Received: 28 November 2015 / Published online: 3 February 2016  
© Springer Science+Business Media New York 2016

**Abstract** This Study synthesized the nanosilver colloid (NSC) via arc discharge. The electric force ionizes the deionized water (DW) inter electrode gap, and the plenty of electrons and ions are attracted by opposite electricity. The electrons and ions strike surface of the electrodes, and sputter the nanosilver particles (NSP). The NSP stably suspend in the DW without surface-active agent. It is a novel and rapid preparation in the standard temperature and pressure. Although the industrial electric discharge machine (EDM) could synthesize NSC, it's too costly and big size. The self-designing micro-EDM that can real-time monitor the processing is substitute the industrial-EDM. By the spectrophotometry, the zetasizer and the scanning electron microscope validate the properties of the NSC that synthesized by the micro-EDM. The results show that the NSC is the same as the features of nanomaterials. The energy of the discharge can be controlled, that can determine the process time. The concentration of the NSP can effectively reduce the difference between the products of the NSC. As the arcing rate ( $A_R$ ) and the absorption peaks are highly correlated, the concentration of the NSP can be predicted during processing. It's a speedy and preliminary determine of the concentration.

**Keywords** Electric discharge machine · Arc discharge · Silver colloid · Nanosilver

## Introduction

Nano-technology is rapid growth in the past few years. It is innovative applications in semiconductor, medical, life, etc. While the size of object is less than 100 nm, the physical phenomenon will differ greatly from the macrostructure [1]. The EDM technique

---

✉ Kuo Hsiung Tseng  
khtseng@ee.ntut.edu.tw

<sup>1</sup> Department of Electrical Engineering, National Taipei University of Technology, Taipei, Taiwan

combined with the nano-technology that successfully synthesized the metallic nanofluid in aqueous solution, such as nanogold [2], nanosilver [3], nanoaluminum [4], and nanotitanium [5]. The discharging sequence is complicated inter electrode gap, and the electrodes are not connected. The discharging current influences the nanoparticles during rising time. Therefore, the different current value will cause the different result [6]. Through the arc discharge prepare the nano colloid whose particles can stably disperse in the DW [7]. Each particle overcomes the Van Der Waals force and the Coulomb force, so the particles are not gathered. In the medical field, the graphite successfully encapsulated gold nanoparticles via arc discharge [8]. It indicated that the arc discharge is a green method, they won't damage the biological.

The principle of using arc discharge to prepare the NSC is to immerse two pure silver electrodes in the DW. The electrodes connect the high frequency pulse repetition, and the gap is controlled by the servo control system. When the width of the gap is about 10  $\mu\text{m}$ , the arc column is produced by the electric field. There are lots of electrons and small amount of ions strike the surface of electrodes. And the kinetic energy converts to the heat energy, that cause the surface temperature is approximately 10,000  $^{\circ}\text{C}$  [9]. Because of high temperature the surface of the electrodes is fused, and much NSP is dispersed in the DW. The current will down to zero during the pulse off-time, and wait for the next pulse on-time. This state is again and again in the processing.

The processing parameters of the EDM effect on the NSP's size and concentration. The following settings are [10]: (1) Pulse on-time ( $T_{\text{on}}$ ): is the total time of spark time and arc time in a period. The power makes the electric field enter the gap. If  $T_{\text{on}}$  is too long, it will cause the rough surface roughness. On the contrary, if  $T_{\text{on}}$  is too short, it will cause the smooth surface roughness. (2) Pulse off-time ( $T_{\text{off}}$ ): cut off the current loop. In order to avoid the state of the centralized discharging, the NSP must be left at the gap, and uniformly dispersed in the DW. (3) Frequency: is the number of the pulses each second. If the frequency is too fast, the charge density is rather low, that two electrodes are not easy to be short circuit. (4) Voltage: determine the value of the electric field strength in the gap. The high voltage can promote discharging stability, but the current is even bigger. (5) Current: flow from the anode to the cathode while the electrodes successfully discharge. If the value of the current is too small, it will produce the smooth surface roughness. Although the smooth surface roughness easily get the small size NSP, the discharging is easy to fail.

The NSP that called the colloid is dispersed in the liquid as a result of the Brownian motion [11]. To prevent the NSP from gathering, it may add chemical substance in the liquid. For example, adjust pH in the liquid [12], add polymer to prevent aggregation [13], and use ultrasound to damage the assemblage of the particles [14]. However, the method of this study only uses pure silver and DW to synthesize the NSC without any chemical substance, then the particles can suspend in the DW for a long time.

The physical phenomenon changes in the nanomaterials field. When the particle size gradually shrinks, the width of energy gap will be inflected. Therefore, under the same element, the optical characteristics are differences in nano and macro. The following instances are: (1) The color is discrepancy between the gold and the nanogold [15]; (2) Coating the NSP on the surface can enhance optical absorption [16]; (3) The size of the  $\text{TiO}_2$  is between 200 and 350 nm that capitally shut out the visible spectrum, and the size of the  $\text{TiO}_2$  is between 15 and 50 nm that capitally shut out the ultraviolet spectrum [17]; (4) The spectrum of particles generally has blue shift. The nanosilver's surface

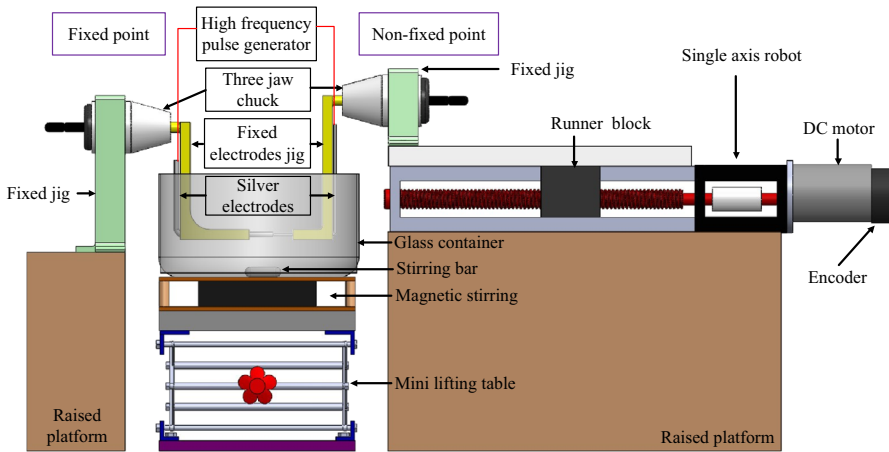


**Fig. 1** The structure of the micro-EDM

plasmon resonance (SPR) absorption peak is at 400 nm. If the size of the particles is smaller, the SPR peak will less than 400 nm. On the contrary, if the size of the particle is bigger, the SPR will more than 400 nm, it's called the red shift [18].

### Materials and Methods

The micro-EDM which follows the principle of the industrial-EDM is designed for preparing the NSP. The structure of the micro-EDM is shown in the Fig. 1. The pure silver be the electrodes that are divided into fixed point and non-fixed point. The non-fixed point is set in the single axis robot. And by the DC motor, it controls the gap under the micrometer scale. The encoder is the signal of the auxiliary DC motor that traces the movement of the runner block, and calculates the electrodes' consumption. The high frequency pulse generator (<50 kHz) connects the electrodes. The glass container collects the NSP and has a stirring bar at the bottom. To disperse the NSP in the DW, the magnetic stirring revolves the stirring bar.

The Fig. 2 is the block diagram of the micro-EDM. The software is called VisSim that is real-time controller/display. And it is based on windows PC. Through the

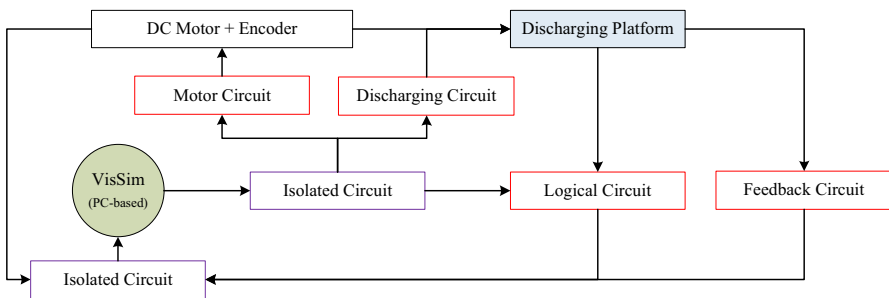


**Fig. 2** The block diagram of the micro-EDM

hardware receive the signals, and command the signals after the VisSim's mathematical operations. The discharging circuit adopts the MOSFET (IRF740) and the power supply (DC-100 V). The MOSFET is a switch which can be controlled the loop to turn-on or turn-off by the VisSim. The gap voltage is captured by the feedback circuit as a feedback value. The command of the motor refers to this feedback value, and keeps the gap in micrometer. The logical circuit retrieves the gap voltage ( $V_{\text{gap}}$ ) and the gap current ( $I_{\text{gap}}$ ). According to the output signal of the logic circuit, the VisSim displays the arcing rate and the energy of the discharge [19].

The  $V_{\text{gap}}$  is distributed into three states. (1) The first state (open circuit): The  $V_{\text{gap}}$  is the maximal value (100 V), and the width of the gap is longer than 50  $\mu\text{m}$ . There is no  $I_{\text{gap}}$  through the gap. (2) The second state (normal discharge): The  $V_{\text{gap}}$  drops down to about 20 V, and the width of the gap is about 10–50  $\mu\text{m}$ . There is  $I_{\text{gap}}$  through the gap. (3) The third state (short circuit): The value of the  $V_{\text{gap}}$  is zero, and two electrodes are almost connected. There is the short circuit current through the gap. The system adopts the optimal discharging value of the  $V_{\text{gap}}$  as the command value ( $V_c$ ). If the  $V_{\text{gap}}$  and the  $V_c$  are equal, it means that the width of the gap is exact, and the runner block is resting. If the  $V_{\text{gap}}$  is more than the  $V_c$ , it means that the width of the gap is too big, and the runner block must be forwarded that two electrodes will close. If the  $V_{\text{gap}}$  is less than the  $V_c$ , it means that the width of the gap is too small, and the runner block must be backed.

The control strategy of the DC motor is proportional-integral-derivative controller (PID-controller), which attempts to minimize the error value (subtract  $V_{\text{gap}}$  from  $V_c$ ). The PID-controller controls the DC motor to forward and reverse, then let the electrodes continuously discharge and produce the NSP. The coefficients of the PID-controller are adjusted by the user. The difference of the coefficients may cause the different discharging effectiveness and the NSC concentration. The Fig. 3a shows the curve of the  $V_{\text{gap}}$  that is stepped-down and integrated. The value is changing during the process. The Fig. 3b shows the curve of the command value

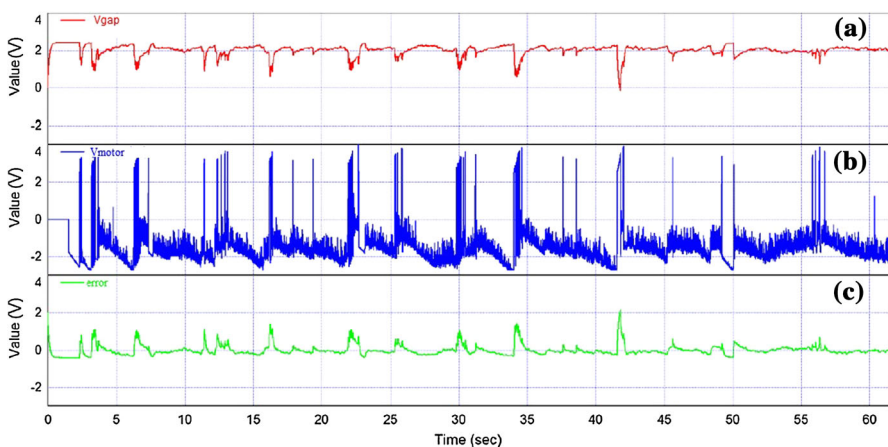


**Fig. 3** a the curve of the  $V_{\text{gap}}$ ; b the curve of the command value of the DC motor; c the curve of the error

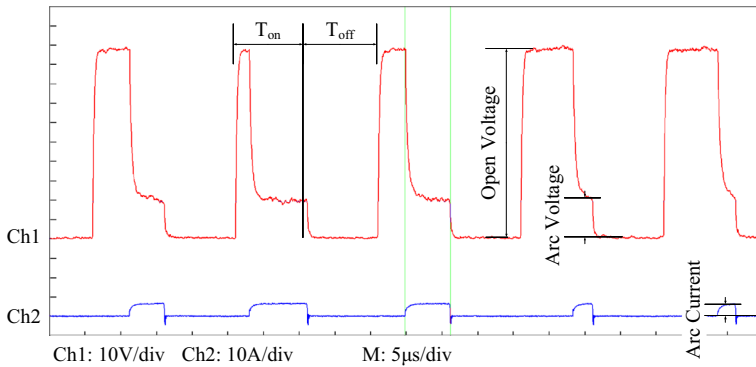


**Fig. 4** The actual waveform of the  $V_{\text{gap}}$  (ch1) and the  $I_{\text{gap}}$  (ch2)

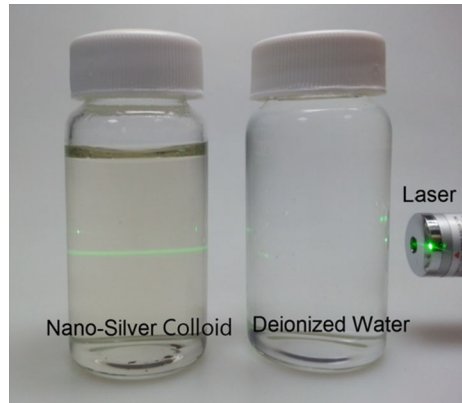
of the DC motor, it presents the motor to sustainably change speed and steering. The Fig. 3c shows the curve of the error. If the value of the error varies smaller, the effectiveness of the processing is higher.

The Fig. 4 is the actual waveform of the  $V_{\text{gap}}$  (Ch1) and the  $I_{\text{gap}}$  (ch2). The open voltage is 100 V, and the arc voltage is about 20 V. The arc current is about 6.4 A. The  $T_{\text{on}}-T_{\text{off}}$  is set as 10–10  $\mu\text{s}$ . When the arc voltage and the arc current occur at meantime, the NSP will be synthesized. There are five periods in the Fig. 4. And every discharging time is different. It shows how the condition of the discharge always changes during the process time. If the process time is assumed to be 60 s, the total time of the discharging and the NSC concentration will be not the same in every preparation. Therefore, this study hopes to reduce the variance of the NSC concentration. Use the energy of the discharge as a condition of the stopping process time and compare to the timer method.

The NSC prepared by the micro-EDM is necessarily validated via the instruments. The following devices are: (1) Laser pen: validate the Tyndall effect. If the volume of particle is less than the wavelength of visible light, it will have the scattering phenomenon [20]. (2) Spectrophotometer (Thermo-Helios Omega): validate the optical character, and find the SPR peak which is proportional to concentration. (3) Malvern zetasizer (Nano-ZS90): validate the surface potential and the size distribution. If the absolute value of the surface potential is greater than 30 mV, the particles perform great suspension [21]. (4) Scanning electron microscope (SEM) and energy dispersive spectrometer (EDS) (Hitachi S-4700): validate the NSP's shape, size, and element.

The main objective of the monitoring system is to get the situation of the discharge. If the arcing rate and the SPR peak are high correlation, the SPR peak can be estimated by arcing rate while the system is running. The Pearson product-moment correlation coefficient is one of the tools in the statistics. It is a measure of the linear correlation between two variables. The absolute value is between 0 and 1 [22]. There are divided into 4 parts: (1) Uncorrelated: 0–0.09; (2) Low correlation: 0.1–0.3; (3) Middle correlation: 0.3–0.5; (4) High correlation: 0.5–1.0. The result of the experiment figures out the coefficient of determination as the predictable equation.

**Fig. 5** The result of the Tyndall effect



For example, the arcing rate as the independent variable, and introduce into the predictable equation. It can get the value of the SPR peak.

## Results and Discussion

### The Characterization of the NSC Prepared by the Micro-EDM

Preparing the NSC need the room temperature, the 200 g deionized water, the pure silver electrodes, the  $T_{\text{on}}-T_{\text{off}}$  setting, and the processing time setting. The Fig. 5 shows the NSC prepared by the micro-EDM (Left bottle) and the deionized water (Right bottle). The  $T_{\text{on}}-T_{\text{off}}$  is 10–10  $\mu\text{s}$  and the process time is 60 s. The result shows that the NSC has a laser beam. It demonstrates that the NSP suspend in the DW.

Although the NSP stably suspend in the DW, there is some particle residue in the bottom of the bottle after the first day. It means that the particles are precipitated since gather. Therefore, this study makes the spectrum of the NSC long-term observation, and then records the SPR peak and the eigenvalue of the wavelength ( $\lambda$ ) every day. The result of the experiment is shown in the Fig. 6. The total time is 49 days. The SPR peak down to 0.19 from 0.222, and the average is 0.192; the  $\lambda$  up to 397 from 392, and the average is 397. The SPR peak is changing violently on the first day. The SPR peak and the  $\lambda$  are stable after the fifth day. The variance percent is less than 3 % that can be regarded as the error of the instrument. The  $\lambda$  of the NSC shows that the spectrum is exactly corresponding to the optical character.

The Fig. 7 is the result of the surface potential and the size distribution. The surface potential is  $-44.8$  mV that indicates the particles perform great suspension as shown in the Fig. 7a. The Fig. 7b is the size distribution whose  $x$ -axis is the particle size, and the  $y$ -axis is the relative intensity. It shows that the range of the intensity is between 1 nm and 10  $\mu\text{m}$ . The size of the NSP is not homogeneous because the energy of the discharge is not the same in the every period. It may cause a small quantity of the bigger NSP suspend in the DW. Therefore, through the SEM

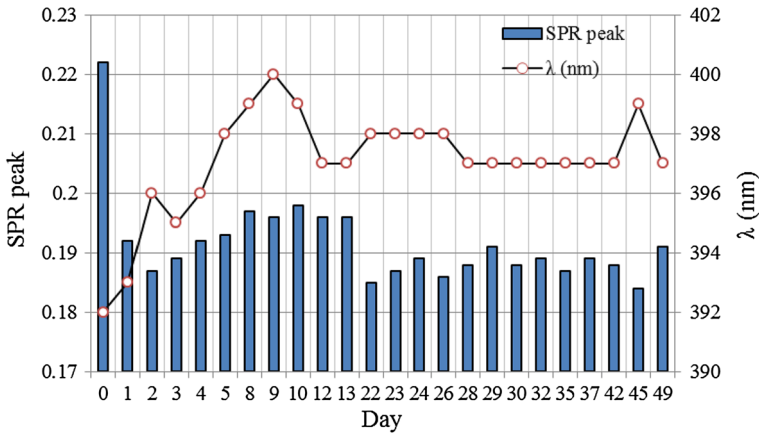


Fig. 6 The spectrum of the NSC

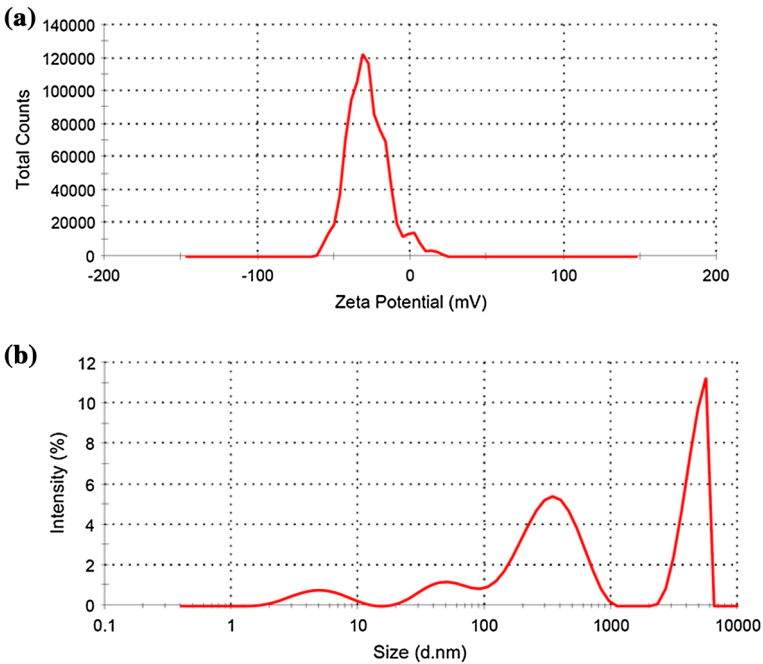
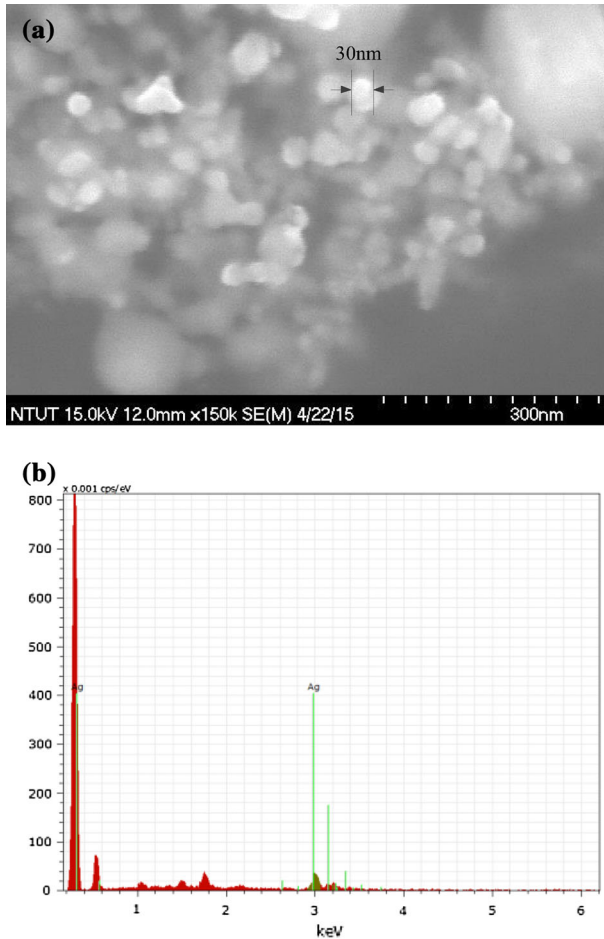


Fig. 7 a the surface potential of the NSC; b the size distribution of the NSC

observes the NSP’s shape, size, and element. The Fig. 8a shows that the size of the NSP is less than 30 nm, and the shape is ellipsoidal. The Fig. 8b shows that the element of the NSC is certainly pure silver.



**Fig. 8** **a** the SEM of the NSC; **b** the EDS of the NSC

### The Condition of the Process Time

In the past, through the timer determines the process time while preparing the NSC. However, the arcing rate is not the same in every time because discharge is the random phenomenon. This section will research the different between the energy of the discharge method and the timer method.

The experimental conditions are below: (1)  $T_{\text{on}}-T_{\text{off}}$ : 10–10  $\mu\text{s}$ ; (2) DW: 200 g; (3) Number of the samples: eighteen. The recording items are SPR peak and arcing rate. The energy of the discharge is set 500 J, and the result is shown in the Fig. 9a. The timer is set 30 s, and the result is shown in the Fig. 9b.



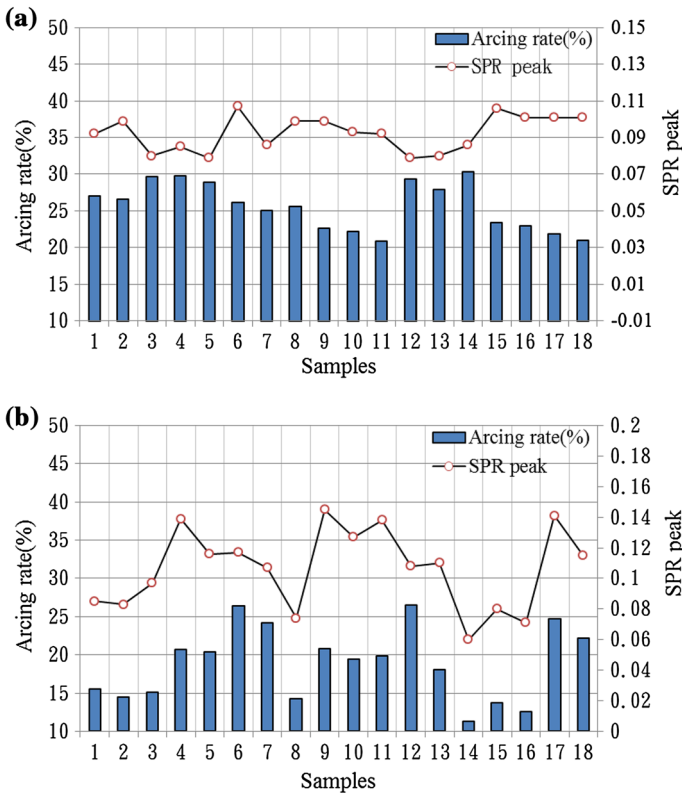


**Fig. 9** a the energy of the discharge mode; b the timer mode

As shown in the Fig. 9a, although the arcing rate of the eleventh and the fourteenth is the most different in every sample, the deviation of the SPR peak is only 0.01. And the average standard deviation of the SPR peak is  $0.093 \pm 0.009$ . It means that the energy of the discharge method can effectively reduce the variation. As shown in the Fig. 9b, the arcing rate is changing violently that also makes the SPR peak is changing violently because the process time is fixed. The average standard deviation of the SPR peak is  $0.106 \pm 0.026$ . According to the result of the experiment, the timer method (Fig. 9b) is not more efficient than the other (Fig. 9a).

**The Correlation Between the Arcing Rate and the SPR Peak**

Using the samples of the Fig. 9b as the object of study since the experimental conditions and the process time are the same. Through the Pearson product-moment correlation coefficient, the value that is 0.742 belongs to the high correlation. The scatter diagram is shown in the Fig. 10. By the exponential fit the trend line. And the

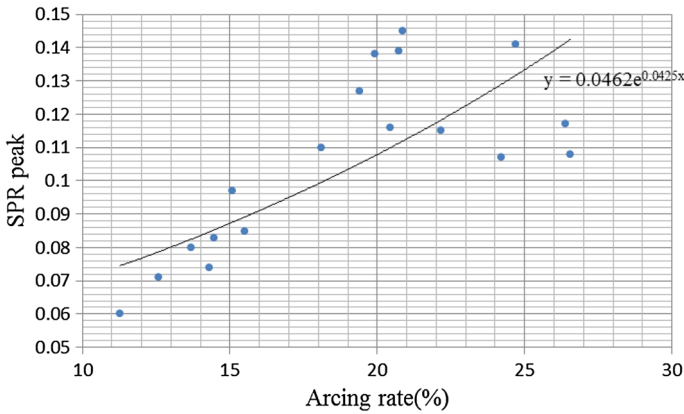


**Fig. 10** The scatter diagram of the SPR peak and the arcing rate

predictable equation is shown in the Eq. (1). This equation can rapidly predict the SPR peak via the arcing rate during the process.

$$y = 0.0462e^{0.0425x} \quad (1)$$

where  $x$  represents the arcing rate, and  $y$  represents the SPR peak.

## Conclusion

This study focuses on the development of the micro-EDM and improves the method of the process. The micro-EDM features are small size, low-cost, and easy operating. The NSP is successfully synthesized by the micro-EDM can suspend in the DW. In order to optimize the process, this study suggests the energy of the discharge method as a condition of the process time. The predictable equation predicts the SPR peak by the arcing rate in the process. The conclusions of this study are as follows:

- A. Developing the whole hardware and software of the micro-EDM. The discharging voltage is 100 V and the discharging current is 6.4 A. The range of the discharging frequency is 0–50 kHz. The gap controller is PID-controller that makes the continuous discharge. The software is VisSim which displays the data in the monitor.
- B. The NSC must be placed for 5 days that the characteristic of the NSC will be stable. The SPR peak is 0.192, the  $\lambda$  is 397 nm, and the surface potential is  $-44.8$  mV. It means that the production exactly correspond to the nanomaterial. Through the SEM image, the particle size is less than 30 nm and the shape is ellipsoidal. It is almost the silver in the DW.
- C. Controlling the energy of the discharge that can effectively reduce the variance of the each NSC. While the arcing rate is low, the process time will be long, and vice versa. Comparing to the timer mode, it is much improved.

- D. While the timer and the parameters are the same, the arcing rate and the SPR peak belong to the high correlation. By the predictable equation estimate the SPR peak in the process. It is faster than the measurement of the UV–Vis.

**Acknowledgments** The authors would like to thank the Ministry of Science and Technology (MOST 103-2221-E-027-070-) for financial supporting this research.

## References

- Jonathan A. Scholl, Aitzol García-Etxarri, Ai Leen Koh, and Jennifer A. Dionne (2013). *Nano Lett.* **13**, 564.
- Kuo-Hsiung Tseng, Chih-Yu Liao, Jen-Chuen Huang, Der-Chi Tien, and Tsing-Tshih Tsung (2008). *Mater. Lett.* **62**, 3341.
- D. C. Tien, C. Y. Liao, J. C. Huang, K. H. Tseng, J. K. Lung, and T. T. Tsung (2008). *Rev. Adv. Mater. Sci.* **18**, 750.
- Chih-Yu Liao, Kuo-Hsiung Tseng, and Hong-Shiou Lin (2013). *Metallu. Mater. Trans. B* **44**, 91.
- Kuo-Hsiung Tseng, Juei-Long Chiu, Heng-Lin Lee, Chih-Yu Liao, Hong-Shiou Lin, and Yi-Syuan Kao (2015). *Adv. Mater. Sci. Eng.* **2015**, 1.
- F. Fang, J. Kennedy, J. Futter, T. Hopf, A. Markwitz, E. Manikandan, and G. Henshaw (2011). *Nanotechnology* **22**, 33.
- R. K. Sahu, S. H. Somashekhar, and P. V. Manivannan (2013). *Proc. Eng.* **64**, 946.
- Enbo Yang and Masaaki Nagatsu (2014). *Jpn. J. Appl. Phys.* **53**, 1.
- Marin Gostimirovic, Pavel Kovac, Milenko Sekulic, and Branko Skoric (2012). *J. Mech. Sci. Technol.* **26**, 173.
- Tushara Prakash, Grant V. M. Williams, John Kennedy, Peter P. Murmu, Jérôme Leveneur, Shen V. Chong, and Sergey Rubanovd (2014). *J. Alloy. Compd.* **608**, 153.
- A. Cuche, B. Stein, A. Canaguier-Durand, E. Devaux, C. Genet, and T. W. Ebbesen (2012). *Nano Lett.* **12**, 4329.
- Ian C. Bourg and Garrison Sposito (2011). *J. Colloid Interface Sci.* **360**, 701.
- Jun Liu, Yangyang Gao, Dapeng Cao, Liqun Zhang, and Zhanhu Guo (2011). *Langmuir* **27**, 7926.
- Jie Lana, Yong Yang, and Xiaochun Li (2004). *Mater. Sci. Eng. A* **386**, 284.
- Kadir Aslana, Joseph R. Lakowicz, and Chris D. Geddesa (2004). *Anal. Biochem.* **330**, 145.
- Yu A Akimov, W. S. Koh, and K. Ostrikov (2009). *Opt. Express* **17**, 10195.
- F. Fang, J. Kennedy, E. Manikandan, J. Futter, and A. Markwitz (2012). *Chem. Phys. Lett.* **521**, 86.
- Majid Darroudi, Mansor Bin Ahmad, Reza Zamiri, A. K. Zak, Abdul Halim Abdullah, and Nor Azowa Ibrahim (2011). *Int. J. Nanomed.* **6**, 677.
- Kuo-Hsiung Tseng, Juei-Long Chiu, Heng-Lin Lee, Yi-Syuan Kao, and Der-Chi Tien (2016). *Mater. Manuf. Process.* **31**, 186.
- Jiunn-Woei Liaw, Shiao-Wen Tsaib, Hung-Hsun Lina, Tzu-Chen Yend, and Bae-Renn Cheng (2012). *J. Quant. Spectrosc. Radiat. Transf.* **113**, 2234.
- Zhaowei Liua, Guogang Renb, Tao Zhangc, and Zhuo Yang (2009). *Toxicology* **264**, 179.
- M. M. Mukaka (2012). *Malawi Med. J.* **24**, 69.